J. Fluid Mech. (1972), *vol.* 55, *part* 4, *pp.* 719–735
Printed in Great Britain

Flow in a deep turbulent boundary layer over a surface distorted by water waves

By A. A. TOWNSEND
Emmanuel College, Cambridge

(Received 31 December 1971)

Linearized equations for the mean flow and for the turbulent stresses over sinusoidal, travelling surface waves are derived using assumptions similar to those used by Bradshaw, Ferriss & Atwell (1967) to compute boundary-layer development. With the assumptions, the effects on the local turbulent stresses of advection, vertical transport, generation and dissipation of turbulent energy can be assessed, and solutions of the equations are expected to resemble closely real flows with the same conditions. The calculated distributions of surface pressure indicate rates of wave growth (expressed as fractional energy gain during a radian advance of phase) of about $15(\rho_a/\rho_w)(\tau_0/c^2)$, where τ_0 is the surface stress, c_0 the phase velocity, and ρ_a and ρ_w the densities of air and water, unless the wind velocity at height $\lambda/2\pi$ is less than the phase velocity. The rates are considerably less than those measured by Snyder & Cox (1966), by Barnett & Wilkerson (1967) and by Dobson (1971), and arguments are presented to show that the linear approximation fails for wave slopes of order 0·1.

1. Introduction

It is only recently that observations of flow velocities and pressures over water waves have been made in sufficient detail to test the several theories that describe their generation. For waves of such small amplitude that the flow may be described by linearized equations, the theory of resonant growth excited by the travelling pressure field of the atmospheric turbulent boundary layer (Phillips 1957) appears to describe the initial growth before the surface deformation has an appreciable effect on the air flow. Then, further growth may be expected through pressure fields induced by the surface deformation, and several attempts to find the exponential rate of growth during the second phase have been presented, starting with the work of Miles (1957). Miles assumed that the undisturbed flow was that in a constant-stress boundary layer and that the Reynolds stresses were not changed by the flow perturbations. The problem is then one of the instability of inviscid flow with the 'turbulent' distribution of mean velocity, and the solution proceeds on well-known lines. In this and subsequent theories of the same kind, considerable importance is attached to flow near the critical layer, at the height where the wind velocity equals the phase velocity of the waves. Here, the fluid moves with the waves and is always exposed to the same increment of distortion rate. It follows that the Reynolds stresses in this region have responded to the wave distortion and are not those of the undisturbed flow.

To include in the theory the effects of the changes of Reynolds stress, it is necessary to make some assumptions about the relation between the mean flow and the turbulent motion, and present knowledge suggests that a good description may be obtained by assuming similarity of the turbulent motion and by use of the equation for the turbulent kinetic energy. The assumptions to be used are not essentially different from those used by Bradshaw *et al.* (1967) for the calculation of boundary-layer development. They are (i) that the ratio of Reynolds stress to total turbulent intensity is everywhere the same, (ii) that the local rate of energy dissipation depends only on the Reynolds stress and on a dissipation length parameter that is proportional to height above the wave surface, (iii) that turbulent kinetic energy is diffused vertically at a rate proportional to its gradient and (iv) that the direction of horizontal Reynolds stress is parallel to the direction of velocity shear.

2. Equations for flow over waves of small amplitude

We consider surface waves propagating at an angle θ to the Ox axis with phase velocity c_0, where the horizontal co-ordinates x, y are chosen so that Ox is in the direction of the undisturbed mean flow $U(z)$ and move relative to the water with velocity $c_0/\cos\theta$ in the Ox direction. In these co-ordinates, the surface displacements are independent of time and given by

$$h = h_0 \exp i(mx+ny), \tag{2.1}$$

where $m = k\cos\theta$, $n = k\sin\theta$ and k is the wavenumber of the surface wave. In this co-ordinate system, mean velocities, Reynolds stresses and mean pressures are also independent of time and, for small amplitudes, vary with the same period as the surface displacement, e.g. $u = u_0 \exp i(mx+ny)$. Writing the deviation of mean velocity from the undisturbed value $U(z)$ as (u, v, w), the Reynolds equations for the mean velocity become, to first order in the fluctuations,

$$\left.\begin{aligned} U\frac{\partial u}{\partial x} + w\frac{\partial U}{\partial z} &= -\frac{\partial}{\partial x}(p-\tau_{zz}) + \frac{\partial \tau_{xz}}{\partial z} + \frac{\partial(\tau_{xx}-\tau_{zz})}{\partial x} + \frac{\partial \tau_{xy}}{\partial y}, \\ U\frac{\partial v}{\partial x} &= -\frac{\partial}{\partial y}(p-\tau_{zz}) + \frac{\partial \tau_{yz}}{\partial z} + \frac{\partial(\tau_{yy}-\tau_{zz})}{\partial y} + \frac{\partial \tau_{xy}}{\partial x}, \\ U\frac{\partial w}{\partial x} &= -\frac{\partial}{\partial z}(p-\tau_{zz}) + \frac{\partial \tau_{xz}}{\partial x} + \frac{\partial \tau_{yz}}{\partial y}, \end{aligned}\right\} \tag{2.2}$$

where p is the pressure fluctuation and τ_{xz}, τ_{yz}, etc., are the fluctuations of the Reynolds stresses. In terms of $P = p - \tau_{zz}$, the equations may be written as

$$\left.\begin{aligned} d\tau_{xz}/dz &= imP + imUu + w\,dU/dz + im(\tau_{zz}-\tau_{xx}) + in\tau_{xy}, \\ d\tau_{yz}/dz &= inP + imUv + in(\tau_{zz}-\tau_{yy}) + im\tau_{xy}, \\ dP/dz &= -imUw + im\tau_{xz} + in\tau_{yz}, \end{aligned}\right\} \tag{2.3}$$

and the condition of incompressibility leads to

$$dw/dz = -imu - inv. \tag{2.4}$$

The next stage is to relate the Reynolds stresses to the mean flow. In the undisturbed flow, the Reynolds stress tensor is symmetrical about the direction of flow, so that $\tau_{xy} = 0$. With a velocity shear in the Oy direction, it is expected that the direction of symmetry, that is the direction of the shear stress, will change towards the direction of the vertical gradient of horizontal velocity. The rapidity of the adjustment is dependent on the 'relaxation' time of the turbulent flow which is of the order of the reciprocal of the rate of shear, $1/(dU/dz)$, and it is likely that the direction of the stress ϕ is described by an equation of the form

$$C_\phi D\phi/Dt = (\phi_0 - \phi)\, dU/dz,$$

where ϕ_0 is the asymptotic value, given by

$$\phi_0 = \frac{dv}{dz}\bigg/\frac{dU}{dz}.$$

For small periodic variations,

$$\phi = \frac{dv}{dz}\bigg/\left(\frac{dU}{dz} + iC_\phi mU\right). \tag{2.5}$$

Naturally, C_ϕ enters only into the calculations for oblique waves.

In addition to the change in horizontal direction of the stress tensor, the ratios of the components may change in the rotated axes, and the turbulent intensity will change over a wave period. The stress ratios in fluid subjected to simple plane hearing appear to be insensitive to increase in the rate of shear, but other kinds of velocity gradient added to a basic plane shearing may cause first-order changes in the ratios. Calculations making the assumption of rapid distortion give a good account of the turbulent structure in ordinary shear flows (Townsend 1970), and table 1 gives the increments in the stress components induced by (*a*) unit plane shear in the Ox direction, (*b*) unit irrotational distortion with the principal positive rate of strain along Ox and (*c*) unit plane shear in the Oz direction, calculated with that assumption for various initial total strains. The calculations refer to the initial *elastic* response and might be directly applicable only in the outer part of the flow, but the characteristic property of increased 'stiffness' to a changed type of shear may well imply that turbulent fluid responds to additional velocity gradients in a strongly anisotropic way. The calculations do not support the use of an isotropic model for the visco-elastic behaviour of turbulent fluid.

If the only changes in the stress tensor are the rotation about the Oz direction and a change in the total intensity, $\overline{q^2} = \overline{u'^2} + \overline{v'^2} + \overline{w'^2}$, the fractional changes in the total normal stresses and in the total shear stress equal the fractional change in total intensity, and the fractional changes in τ_{yz} and τ_{xy} are equal to ϕ. If the stresses in the undisturbed flow are written as

$$\tau_{yz} = -a_{yz}\overline{q^2}, \text{ etc.,}$$

the result is that the stress changes are

$$\left.\begin{aligned} \tau_{xx} &= a_{xx}(\overline{q^2})', \quad \tau_{yy} = a_{yy}(\overline{q^2})', \quad \tau_{zz} = a_{zz}(\overline{q^2})', \\ \tau_{xz} &= a_{xz}(\overline{q^2})', \quad \tau_{yz} = a_{xz}\overline{q^2}\phi, \quad \tau_{xy} = (a_{yy} - a_{xx})\,\overline{q^2}\,\phi. \end{aligned}\right\} \tag{2.6}$$

Increment	Component	Initial total shear ratio 1·0	2·0	3·0	4·0
Ox shear	τ_{xx}	−0·57	−1·11	−1·63	−1·95
	τ_{xz}	0·39	0·32	0·25	0·13
	τ_{zz}	0·16	0·14	0·16	−0·06
Irrotational	τ_{xx}	1·47	3·28	6·03	9·54
	τ_{xz}	0·02	0·07	0·08	0·42
	τ_{zz}	−0·73	−0·68	−0·64	−0·74
Oz shear	τ_{xx}	0·23	0·54	1·02	1·68
	τ_{xz}	0·46	0·65	0·88	1·04
	τ_{zz}	−0·53	−0·85	−0·93	−1·05

Note that the incremental strain tensors are

$\begin{pmatrix} 0 & 1 \\ 0 & 0 \end{pmatrix}$ for Ox shear, $\begin{pmatrix} 1 & 0 \\ 0 & -1 \end{pmatrix}$ for irrotational shear, $\begin{pmatrix} 0 & 0 \\ 1 & 0 \end{pmatrix}$ for Oz shear.

TABLE 1. Reynolds stress components induced by incremental strains of sheared turbulence

So the changes in Reynolds stress are described by the angle ϕ and by $(\overline{q^2})'$, the change in total intensity. The change in ϕ is given by equation (2.5).

The change in total intensity is found from the equation for the turbulent kinetic energy. Omitting second-order terms, it becomes

$$U\frac{\partial(\frac{1}{2}\overline{q^2})'}{\partial x}+\frac{\partial}{\partial z}(\overline{p'w'}+\tfrac{1}{2}\overline{q^2w'}) = \tau_{xz}\frac{dU}{dz}+\tau_0\frac{du}{dz}-\epsilon', \tag{2.7}$$

where ϵ' is the change in dissipation rate caused by the waves. To use it as an equation for the stresses, assumptions must be made about the diffusion term and the dissipation term. The vertical flux of energy will be assumed proportional to the gradient with a diffusion coefficient that is a constant fraction of the eddy viscosity for the undisturbed flow, i.e. $K\tau_0^{\frac{1}{2}}z$, where τ_0 is the constant shear stress. Then the diffusive flux is

$$\overline{p'w'}+\tfrac{1}{2}\overline{q^2w'} = -DK\tau_0^{\frac{1}{2}}z(d\tau_{xz}/dz)/2a_{xz}. \tag{2.8}$$

Next, the total dissipation is assumed to be given by

$$\epsilon = (\overline{q^2})^{\frac{3}{2}}/L_\epsilon, \tag{2.9}$$

where L_ϵ is proportional to 'height above the wave surface'. Physically, the variation must arise from the constriction of eddy size by the presence of an impermeable boundary and, very close to the surface, the length is certainly proportional to $z-h$. At heights comparable with or greater than the wave-length, the constriction is by a considerable area of surface and L_ϵ will be more nearly proportional to height above the average position of the surface. It appears reasonable to represent the behaviour by assuming that

$$L_\epsilon = (K/a_{xz}^{\frac{3}{2}})(z-h\,e^{-kz}), \tag{2.10}$$

where the factor is chosen to allow energy balance in the undisturbed flow.† Then the change in dissipation rate is, to first order,

$$\epsilon' = \frac{3}{2}\frac{\tau_0^{\frac{1}{2}}}{Kz}\tau_{xz} + \frac{\tau_0^{\frac{3}{2}}}{Kz^2}h\,e^{-kz} \tag{2.11}$$

and the energy equation becomes

$$\frac{im}{2a_{xz}}U\tau_{xz} + \tfrac{1}{2}U'\tau_{xz} - \frac{KD\tau_0^{\frac{1}{2}}}{2a_{xz}}\frac{d}{dz}\left(z\frac{d\tau_{xz}}{dz}\right) = -\frac{\tau_0^{\frac{3}{2}}}{Kz^2}e^{-kz}h + \tau_0\frac{du}{dz}. \tag{2.12}$$

The equations (2.3)–(2.6) and (2.12) are a set of inhomogeneous linear equations for τ_{xz}, τ_{yz}, P, u, v and w in an undisturbed flow specified by $U(z)$. If the effective roughness length of the surface is z_0, the velocity distribution is

$$U = (\tau_0^{\frac{1}{2}}/K)\log(z/z_0) - kc_0/m. \tag{2.13}$$

At this stage, it is convenient to describe the flow in variables made non-dimensional by use of a velocity scale $\tau_0^{\frac{1}{2}}$ and a length scale k^{-1}. In the non-dimensional representation, the flow depends on the non-dimensional parameters $R = -\log(kz_0)$, $C = c_0/\tau_0^{\frac{1}{2}}$ and θ, and is linearly dependent on the maximum slope kh_0 of the wave surface.

3. Boundary conditions of the flow

For numerical solution of the flow equations it is necessary to set boundary conditions at the inner and outer limits of the integration. The outer conditions depend on the requirement that the flow disturbance becomes small for large values of the non-dimensional height. There the changes in Reynolds stress have a negligible effect on the flow and the non-dimensional equations reduce to

$$\left.\begin{aligned} 0 &= imP + imUu + w\,dU/dz,\\ 0 &= inP + imUv,\\ dP/dz &= -imUw,\\ dw/dz &= -imu - inv. \end{aligned}\right\} \tag{3.1}$$

After elimination of u, v and P, these yield

$$d^2w/dz^2 = (1 + U''/U)\,w \tag{3.2}$$

(where primes indicate differentiation with respect to z), and, if

$$U/U'' = z^2[\log(z/z_0) - KC/m]$$

is large, the solution of (3.2) that becomes small for large z is very nearly

$$w = w_0 e^{-z}. \tag{3.3}$$

Then, from (3.1),

$$\left.\begin{aligned} P &= imU[1 + U'/U]\,w,\\ u &= -im[1 - (n^2/m^2)\,U'/U]\,w,\\ v &= -in[1 + U'/U]\,w, \end{aligned}\right\} \tag{3.4}$$

where the (square) bracketed expressions are nearly one.

† If the flow were irrotational, the factor could be justified.

Equations (3.4) provide three conditions that must be satisfied at the outer boundary, and three inner conditions are necessary to determine a solution. The energy equation (2.12) is applicable only within the turbulent flow and the integration must not be carried to values of z that lie within the viscous layer of the flow. In general, the viscous layer is thin and the integration can extend so close to the surface that the velocity distribution is nearly that of a constant-stress equilibrium layer. Allowing for the orbital velocity of the wave motion, the velocities are given by the logarithmic expressions

$$\left.\begin{aligned} U+u &= \frac{\tau_{xz}^{\frac{1}{2}}}{K}\log\left(\frac{z-h}{z_0}\right)+mCh-C/m, \\ v &= \frac{\tau_{yz}}{K\tau_{xz}^{\frac{1}{2}}}\log\left(\frac{z-h}{z_0}\right)+nCh, \end{aligned}\right\} \tag{3.5}$$

where the stresses are values at the surface. To first order in h, the fluctuations are given by

$$\left.\begin{aligned} u &= (1/2K)\,(\tau_{xz})_0\log(z/z_0)+mCh-h/Kz, \\ v &= (1/K)\,(\tau_{yz})_0\log(z/z_0)+nCh, \end{aligned}\right\} \tag{3.6}$$

where $(\tau_{xz})_0$ and $(\tau_{yz})_0$ are the stress fluctuations at the surface. Using the continuity equation and assuming validity of the logarithmic profiles, it may be shown that

$$\begin{aligned} w = i(mU-Cz)\,h-(imz/2K)\,(\log z/z_0-1)\,(\tau_{xz})_0 \\ -(inz/K)\,(\log z/z_0-1)\,(\tau_{yz})_0. \end{aligned} \tag{3.7}$$

Although the inner boundary may be very close to the surface, it is not accurate to put the surface stresses equal to the Reynolds stresses at the inner boundary. The difference is found by the equation of mean flow through the equilibrium layer, i.e.

$$\left.\begin{aligned} \frac{\partial\tau_{xz}}{\partial z} &= \frac{\partial P}{\partial x}+U\frac{\partial U}{\partial x}+V\frac{\partial U}{\partial y}+W\frac{\partial U}{\partial z}, \\ \frac{\partial\tau_{yz}}{\partial z} &= \frac{\partial P}{\partial y}+v\frac{\partial V}{\partial x}+V\frac{\partial V}{\partial y}+W\frac{\partial V}{\partial z}, \end{aligned}\right\} \tag{3.8}$$

or, in terms of the fluctuations,

$$\left.\begin{aligned} \tau_{xz}-(\tau_{xz})_0 &= imPz+\frac{iz}{2K^2}\left(m\log^2\frac{z}{z_0}-(3m+Kc_0)\log\frac{z}{z_0}+4m+Kc_0\right)(\tau_{xz})_0 \\ &\quad -\frac{inz}{K^2}\left(\log\frac{z}{z_0}-2\right)(\tau_{yz})_0+\frac{ic_0z}{K}\left(m^2\left(\log\frac{z}{z_0}-1\right)-1-Kmc_0\right)h, \\ \tau_{yz}-(\tau_{yz})_0 &= inPz+\frac{iz}{2K^2}\left(m\log^2\frac{z}{z_0}-(2m+Kc_0)\log\frac{z}{z_0}+2m+Kc_0\right)(\tau_{yz})_0 \\ &\quad +\frac{inc_0z}{K}\left(m\log\frac{z}{z_0}-m-Kc_0\right)h. \end{aligned}\right\} \tag{3.9}$$

The conditions expressed by (3.6), (3.7) and (3.9) are sufficient to make the problem of integration determinate. The procedure has been to integrate the flow equations inwards from a sufficiently distant outer boundary with trial values of w, τ_{xz} and τ_{yz}, and values of P, u, v given by equations (3.4), and then to add to this particular solution a linear combination of solutions of the homogeneous equations (i.e. omitting the term $-e^{-z}h/Kz^2$ in (2.12)) chosen so that the composite solution satisfies the inner conditions as well as the outer ones. By varying the inner and outer limits of the integration (usually by factors of two), it was possible to verify that their choice had little effect on the solution. For large positive values of $c_0/U(k^{-1})$, the outer limit had to be increased, but the normal limits of kz were 3 and $e^{-4} = 0{\cdot}0183$.

4. Results of the calculations

For completeness, the flow equations in § 2 include all components of the Reynolds stress, but trials have shown that the calculated solutions are not significantly different if stresses other than τ_{xz} and τ_{yz} are ignored. All the following results have been calculated on this basis. Besides the Kármán constant $K = 0{\cdot}41$, the equations contain three constants characteristic of turbulent wall flow. The first and most important is the stress-intensity ratio $a_{xz} = \tau_{xz}/\overline{q^2}$ (a_1 in the notation of Bradshaw, Ferriss & Atwell), and it is assumed that $a_{xz} = 0{\cdot}15$. The second constant describes the magnitude of vertical diffusion of turbulent energy by an eddy diffusivity (equation (2.8)), and it occurs in the combination $DK/2a_{xz}$. Using an eddy diffusivity in the energy equation for a zero-stress equilibrium layer (Townsend 1961), it may be shown that $dU/dz = \tau^{\frac{1}{2}}/K_0 z$, where

$$K_0 = K/(1-B) \quad \text{and} \quad B = \tfrac{3}{4}K^2D/a_{xz}.$$

The available evidence suggests that $B \simeq 0{\cdot}2$, indicating that $DK/2a_{xz} \simeq 0{\cdot}32$. Most of the results presented are for $DK/2a_{xz} = 0{\cdot}3$, but trials have shown that surface values of pressure are almost independent of the constant over the range 0·1–0·5. The third constant allows for lag in the adjustment of the principal axes of the Reynolds stress tensor to the changing direction of shear (equation (2.5)) and, in the absence of any measurements, it has been set equal to one.

For the problem of wave generation, the important quantities are the amplitudes of the pressure and shear stress fluctuations over the wave surface. For example, the horizontal stress exerted on the water by the pressure field is

$$\tau_w(0) = \tfrac{1}{2}P_i(kh_0)^2\tau_0, \tag{4.1}$$

where kh_0 is the maximum wave slope. Surface pressures and stresses are given as non-dimensional coefficients in table 2 for the wind direction normal to the wave fronts. Some additional entries show the insensitivity of surface values to the magnitude of the diffusion parameter or to the nature of the surface roughness. From figure 1, it can be seen that P_i, the imaginary component of the pressure amplitude, increases with $c_0/U(k^{-1}) \equiv KC/R$ to a peak value of about $22kh_0\tau_0$ for $c_0/U(k^{-1}) \simeq 0{\cdot}8$, and then decreases rapidly to small negative values. The phase of the pressure fluctuation (relative to the wave height) is nearly 180° except for $c_0/U(k^{-1}) = 0{\cdot}6$–$0{\cdot}8$ when it is nearer to 90°. The amplitudes of stress variation are in the range 2–$5kh_0\tau_0$, and the phase increases from about 30° to

R	KC/R	P_r	P_i	τ_r	τ_i	$\phi_p/2\pi$
8	0	−262·0	11·02	4·28	1·69	—
8	0·205	−145·4	10·37	2·99	1·54	0·489
		(−148·1	0·0	2·91	−0·93)	
8	0·375	−98·65	10·67	2·36	1·58	—
		(−98·65	11·16	2·40	1·59)	
8	0·41	−59·85	11·84	1·70	1·71	0·469
		(−59·87	11·83	1·71	1·68)	
8	0·512	−29·58	14·40	0·94	1·96	—
		(−29·59	14·32	0·96	1·93)	
8	0·615	−9·54	18·41	−0·04	2·23	0·326
		(−9·44	18·25	0	2·20)	
8	0·718	−2·06	21·54	−1·24	2·28	—
		(−1·67	21·51	−1·19	2·28)	
8	0·82	−6·44	18·42	−2·37	1·98	0·303
		(−6·09	19·03	−2·35	2·03)	
8	0·922	−14·28	2·11	−3·17	1·37	—
		(−15·35	2·79	−3·24	1·34)	
8	1·025	−5·16	−1·12	−3·31	1·38	0·534
		(−2·33	−2·00	−3·31	1·34)	
8	1·281	−64·04	−1·29	−4·99	1·79	—
8	1·538	−169·8	−2·60	−6·85	2·29	—
10	0·164	−287·6	8·73	2·96	1·10	0·495
10	0·205	−253·8	8·64	2·73	1·09	—
10	0·328	−164·2	8·88	2·03	1·11	—
		(−166·6	9·17	2·64	1·51)*	
10	0·41	−114·0	9·68	1·57	1·19	0·469
10	0·492	−71·86	11·43	1·07	1·34	—
		(−73·6	10·36	1·42	1·70)*	
10	0·615	−25·22	16·89	0·13	1·68	—
10	0·656	−15·05	19·36	−0·29	1·78	0·355
		(−14·22	17·03	−0·17	2·34)*	
10	0·82	−5·16	21·40	−2·11	1·53	0·288
		(−4·75	21·80	−2·08	1·57)	
		(−2·52	23·30	−2·67	2·47)*	
10	0·984	(−8·97	−8·88	−3·95	1·43)*	—
12	0·171	−434·4	7·23	2·70	0·79	0·497
12	0·205	−393·8	7·44	2·60	0·86	—
12	0·342	−247·4	7·13	1·78	0·79	0·495
12	0·41	−186·1	7·54	1·42	0·83	—
12	0·512	−108·6	9·31	0·88	0·97	0·486
12	0·684	−22·28	18·85	−0·37	1·45	0·388
12	0·854	−6·52	21·01	−2·19	1·16	0·298
12	1·025	−8·37	1·59	−2·85	0·65	0·470

Note that simple brackets indicate results for a diffusion factor $DK/(2a_{xz})$ of 0·1 rather than 0·3. Brackets with an asterisk indicate results for roughness length proportional to local shear stress.

TABLE 2. Non-dimensional amplitudes of pressure and stress

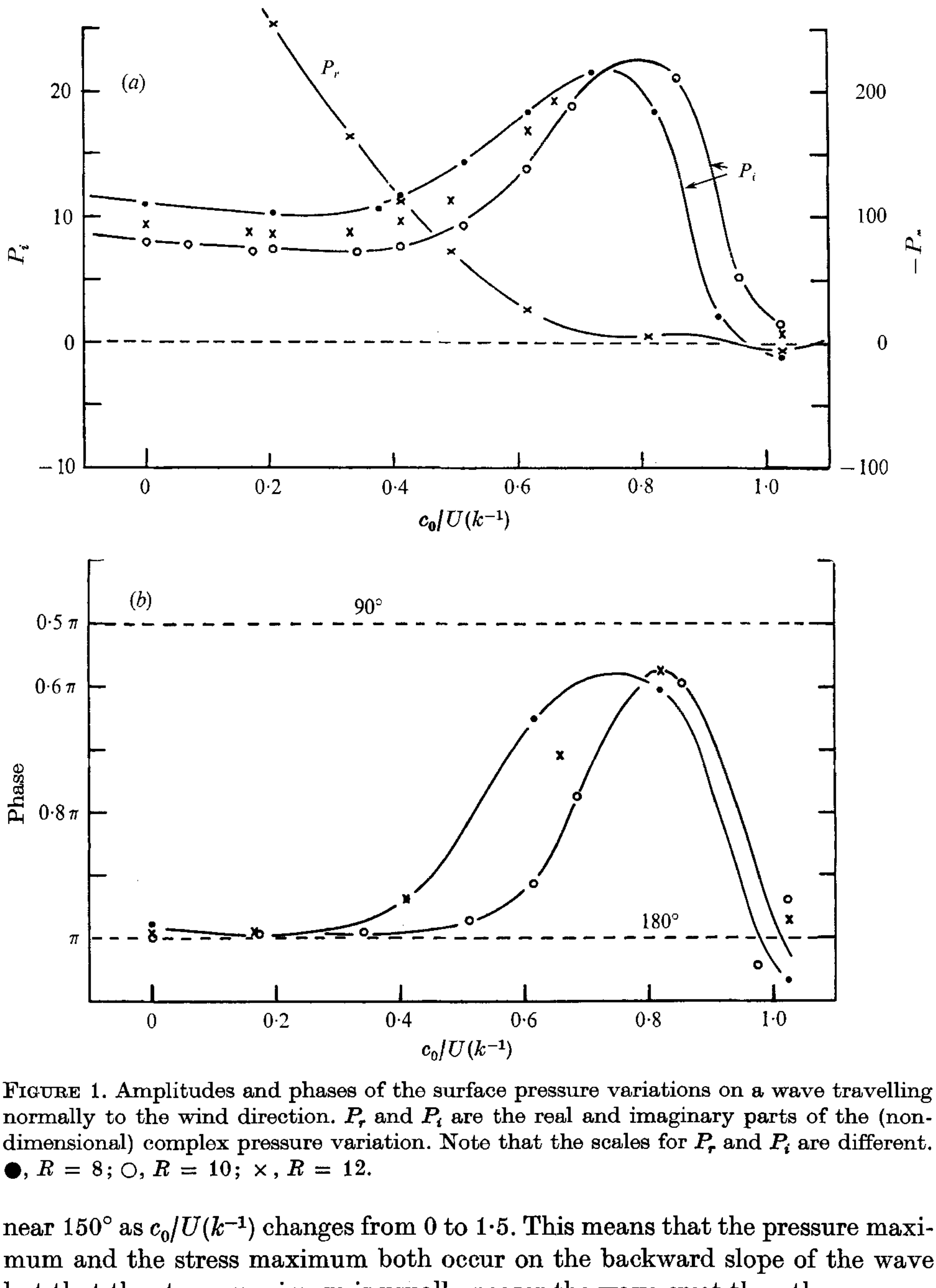

FIGURE 1. Amplitudes and phases of the surface pressure variations on a wave travelling normally to the wind direction. P_r and P_i are the real and imaginary parts of the (non-dimensional) complex pressure variation. Note that the scales for P_r and P_i are different. ●, $R = 8$; ○, $R = 10$; ×, $R = 12$.

near 150° as $c_0/U(k^{-1})$ changes from 0 to 1·5. This means that the pressure maximum and the stress maximum both occur on the backward slope of the wave but that the stress maximum is usually nearer the wave crest than the pressure maximum, especially for smaller $c_0/U(k^{-1})$.

Table 3 and figure 2 show surface pressures and stresses for a wind direction at an angle to the wave normal. Their magnitudes are approximately the same as for zero angle if the wind velocity resolved normal to the wave front is used as a scale, i.e. $P/(mU(k^{-1}))^2$ is dependent mostly on the value of $c_0/U(k^{-1})\,m$ and hardly at all on $m = \cos\theta$ (θ is the angle between the wind and the wave normal).

R	m	KC/mR	P Real	P Imag.	τ_{xz} Real	τ_{xz} Imag.	τ_{yz} Real	τ_{yz} Imag.
8	0·8	0·256	−77·64	6·89	1·95	1·02	0·50	0·30
8	0·8	0·320	−60·17	7·12	1·73	1·07	0·37	0·26
8	0·8	0·512	−19·48	8·81	0·91	1·48	0·04	0·18
8	0·8	0·641	−4·05	11·41	−0·03	1·88	−0·05	0·11
8	0·8	0·770	−1·16	13·17	−1·46	1·57	−0·15	0·48
8	0·8	1·025	−4·65	−3·54	−2·00	0·88	−0·90	0·24
8	0·5	0·410	−15·68	3·01	1·10	0·67	0·14	0·18
8	0·5	0·488	−8·27	3·17	0·95	0·88	0·14	0·18
8	0·5	0·820	−0·63	4·41	−1·16	0·85	−0·21	0·42
8	0·5	1·230	−12·51	−0·50	−0·55	0·72	−1·10	0·36
8	0·5	1·640	−56·19	−1·19	−1·52	0·79	−1·75	0·38
10	0·8	0·102	−218·6	5·91	2·25	0·70	0·74	0·23
10	0·8	0·205	−162·4	5·75	1·90	0·69	0·56	0·21
10	0·8	0·410	−73·3	6·33	1·23	0·82	0·21	0·18
10	0·8	0·615	−16·59	10·06	0·33	1·32	−0·09	0·10
10	0·8	0·820	−2·60	13·46	−1·58	1·01	−0·32	0·42
10	0·8	1·025	−3·93	−2·52	−1·82	0·59	−0·79	0·15
10	0·5	0·164	−72·0	2·67	1·13	0·22	0·51	0·19
10	0·5	0·328	−41·42	2·61	0·98	0·34	0·27	0·16
10	0·5	0·492	−18·67	2·87	0·82	0·53	0·04	0·12
10	0·5	0·656	−4·23	3·76	0·48	0·97	−0·15	0·06
10	0·5	0·985	−3·34	−1·02	−0·28	0·45	−0·71	0·10
12	0·8	0·171	−277·8	4·75	1·83	0·49	0·58	0·15
12	0·8	0·342	−158·5	4·80	1·29	0·51	0·32	0·14
12	0·8	0·512	−70·0	6·02	0·76	0·68	0·05	0·13
12	0·8	0·683	−14·56	11·09	−0·04	1·17	−0·17	0·07
12	0·8	0·853	−3·48	13·22	−1·57	0·71	−0·41	0·34
12	0·5	0·137	−119·3	2·39	0·99	0·16	0·52	0·14
12	0·5	0·274	−79·22	2·21	0·86	0·19	0·34	0·13
12	0·5	0·410	−46·86	2·25	0·75	0·25	0·16	0·12
12	0·5	0·547	−22·37	2·64	0·64	0·41	−0·02	0·10
12	0·5	0·684	−6·14	3·69	0·40	0·76	−0·18	0·05
12	0·5	0·820	0·02	5·44	−0·63	1·02	−0·19	0·10

TABLE 3. Pressure and stress amplitudes for oblique incidence

Profiles of pressure, stress and velocity amplitudes were obtained in the course of the calculations, and sample profiles are shown in figures 3–5. Over the interesting range of $c_0/U(k^{-1})$, 0 to 0·8, the phase of the pressure fluctuation and the vertical component of velocity hardly change through the layer of modified flow, but the profiles of Reynolds stress show the expected 'diffusive' wave with at least two phase reversals. As a rule, the stress amplitude at the height of phase reversal relative to the surface stress is similar to the amplitude at the surface, and, in typical conditions (say for $R = 10$, $C = 10$) the difference of stress may be near $4kh_0\tau_0$. For a wave slope of 0·1, the stress at the height of phase reversal is calculated as 50 % greater than the surface value near minimum surface stress, and it is likely that the flow may not be accurately described by the linearized equations.

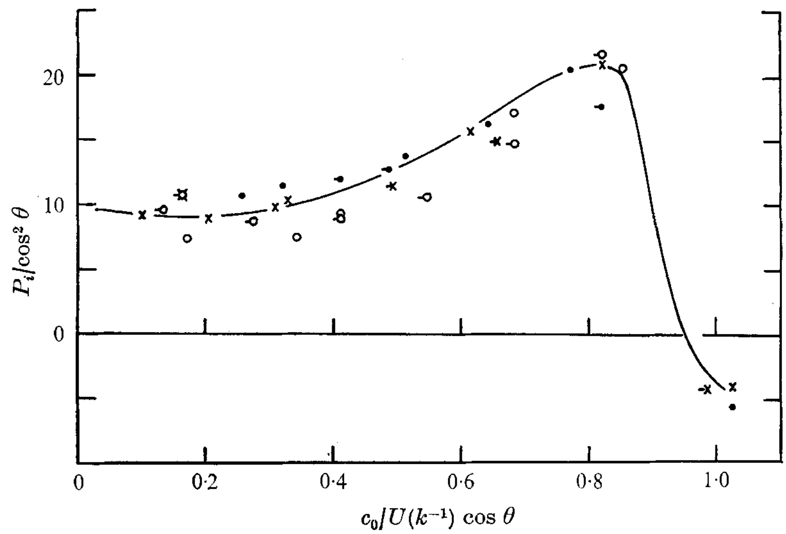

FIGURE 2. Imaginary parts of the complex pressure variations on waves travelling at an angle to the wind direction. ●, $R = 8$; ○, $R = 10$; ×, $R = 12$. Plain points are for $\cos\theta = 0{\cdot}8$, tailed points for $\cos\theta = 0{\cdot}5$. Note the scale factors of $\cos\theta$ and $\cos^2\theta$ on the abscissae and ordinates.

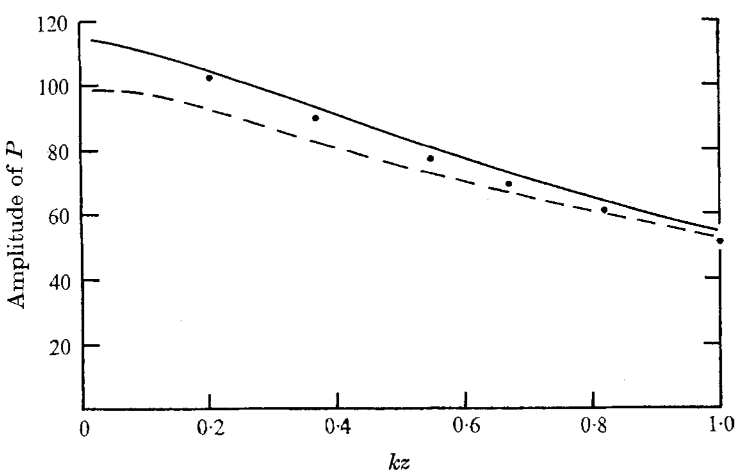

FIGURE 3. Variation of pressure amplitude with distance from surface for $R = 10$ and $C = 4, 10, 16$. The moduli are plotted. The phases remain nearly constant, i.e. for $C = 4$, $\phi = 0{\cdot}990\pi$, for $C = 10$, $\phi = 0{\cdot}974\pi$ and for $C = 16$, $\phi = 0{\cdot}710\pi$–$0{\cdot}714\pi$. ●, $C = 4$ ($\times 0{\cdot}4$); ——, $C = 10$; – – –, $C = 16$ ($\times 4$).

A quantity of considerable interest is the local wave stress, that is the rate of downward transfer of momentum by the periodic motion induced by the waves. Since the horizontal flow velocity averaged over horizontal planes is unchanging, the total vertical flux of momentum is the same at all heights and, accordingly,

$$\tau_\infty = \tau_0 + \tau_w, \tag{4.2}$$

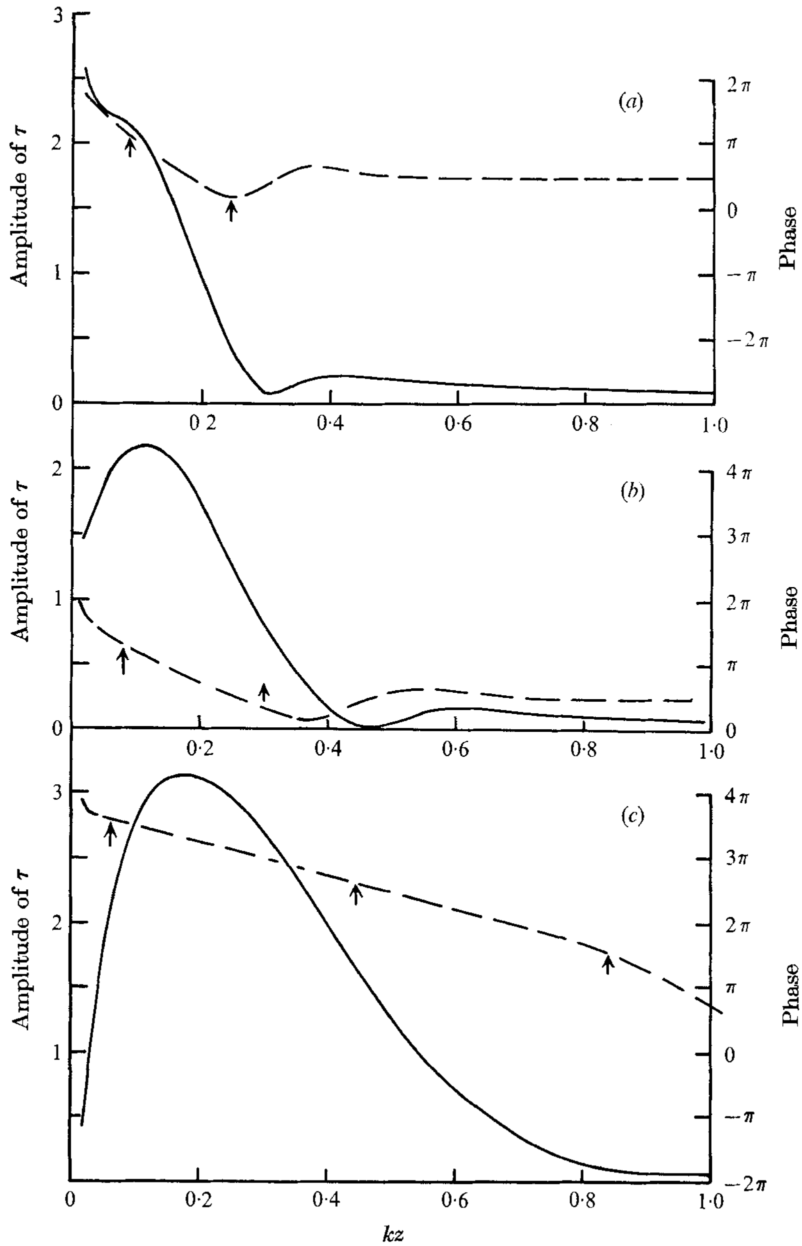

FIGURE 4. Variation of Reynolds stress amplitude with distance from surface for $R = 10$ and (*a*) $C = 4$, (*b*) $C = 10$ and (*c*) $C = 16$. Moduli (solid lines) and phases (broken lines) are plotted. Arrows indicate positions of phase reversal relative to phase of wall stress variation.

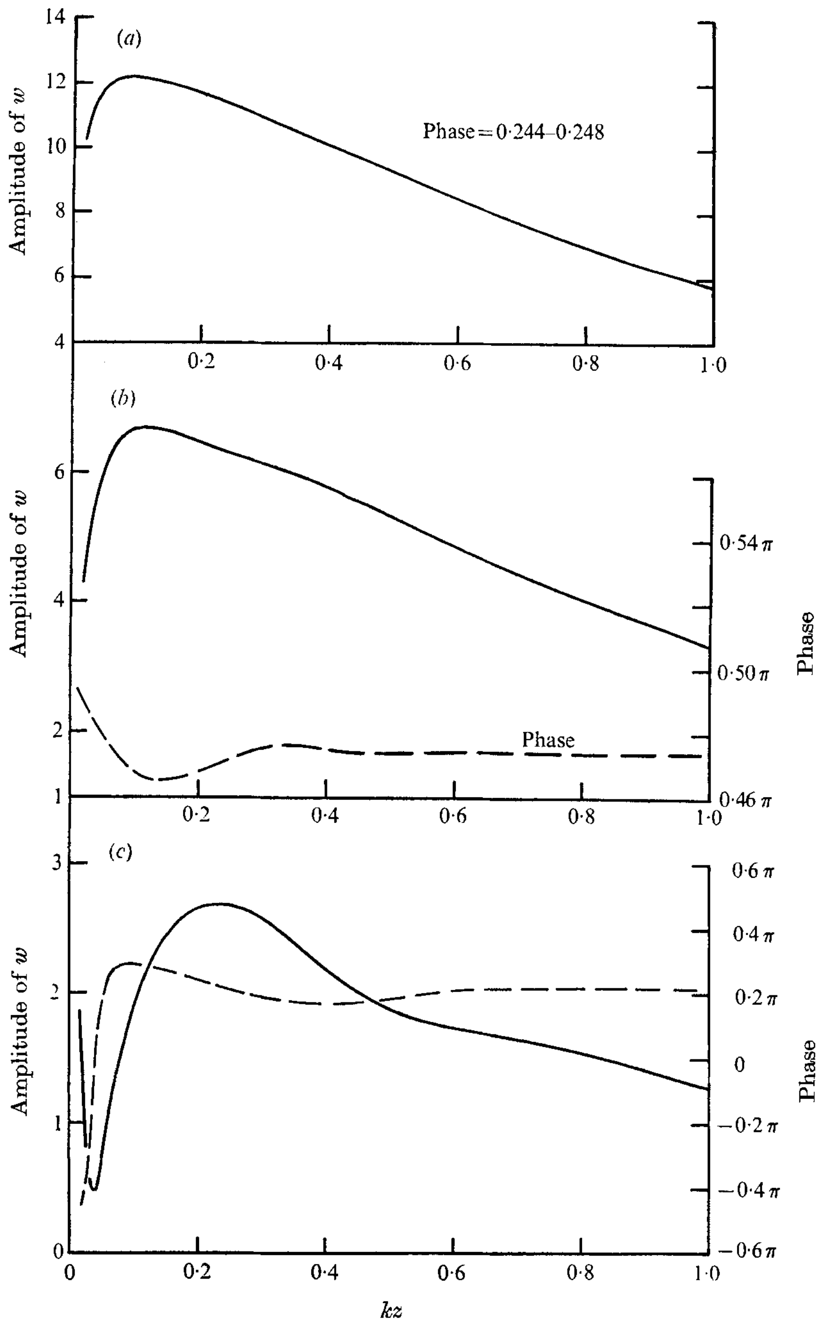

FIGURE 5. Variation of amplitude of vertical velocity component with distance from surface for $R = 10$ and (*a*) $C = 4$, (*b*) $C = 10$ and (*c*) $C = 16$. Moduli (solid lines) and phases (broken lines) are plotted.

where τ_∞ is the Reynolds stress far above the waves, τ_0 is the horizontally averaged Reynolds stress and τ_w is the wave stress, given by

$$\tau_w = \tfrac{1}{4}(kh_0)^2 \tau_0 (uw^* + u^*w), \tag{4.3}$$†

where u and w are the non-dimensional complex amplitudes of the velocity fluctuations. Some profiles of the non-dimensional wave stress $\frac{1}{2}(uw^* + u^*w)$ are shown in figure 6. They indicate that the wave stress becomes negative very close to the surface and attains a large negative value near the position where the stress fluctuations have reversed in phase. Above it continues to oscillate with diminishing amplitude. The magnitude of the variations is such that the basic stress distribution will be considerably changed from uniformity if the wave slope exceeds 0·1.

5. Discussion

The calculated values of the quadrature component of the pressure variation, which determines the energy transfer from the wind to the waves, are similar in magnitude to those given by Miles (1959), who neglected Reynolds stresses entirely. For example, the maximum value of P_i, nearly 22 in figure 1, can be compared with maximum values near 20 for comparable values of Reynolds number, i.e. of $1/(kz_0)$.‡ The main difference is that the maximum is more pronounced in figure 1 of this paper than it is in figure 4 of Miles's paper. It is surprising that the differences are not larger since the critical layer where wind and phase velocities are equal is of central importance in stability theory while it is merely an unimportant part of an equilibrium layer if turbulent stresses are included through the turbulent energy equation. The reason is that the turbulent flow near the critical layer is not subjected to periodic changes in the rate of shear, and it is able to develop an equilibrium structure appropriate to the local rate of shear. Indeed, for many of the calculations, the critical height lay outside the range of numerical integration and within the region described by the inner boundary conditions (3.6) and (3.7).

Although the attention paid to the turbulent motion makes for a more realistic account of the flow, the linearized theory is not able to account for the considerable discrepancy between calculated surface pressures and those measured in recent field studies by Snyder & Cox (1966)§ and by Dobson (1971). It is possible that some allowance for the changes in stress ratios caused by the wave flow might improve the agreement but the extremely small effect produced if normal stresses are included in the calculation makes this doubtful. Recently, Davis (1972) has concluded that the visco-elastic response of turbulent fluid to changes of strain may be sufficient to account for the discrepancy between the observations and predictions assuming either zero viscosity or an eddy viscosity (Hussain &

† Note that u^* is the complex conjugate of the velocity $u_0 \exp i(mx + ny)$, *not* the friction velocity.

‡ In Miles's notation, $P_i = \beta_i / K^2$.

§ Snyder & Cox measured the growth rates of the waves, not the pressures, and the statement refers to the imaginary components of the pressure fluctuations necessary to induce the observed growth rates.

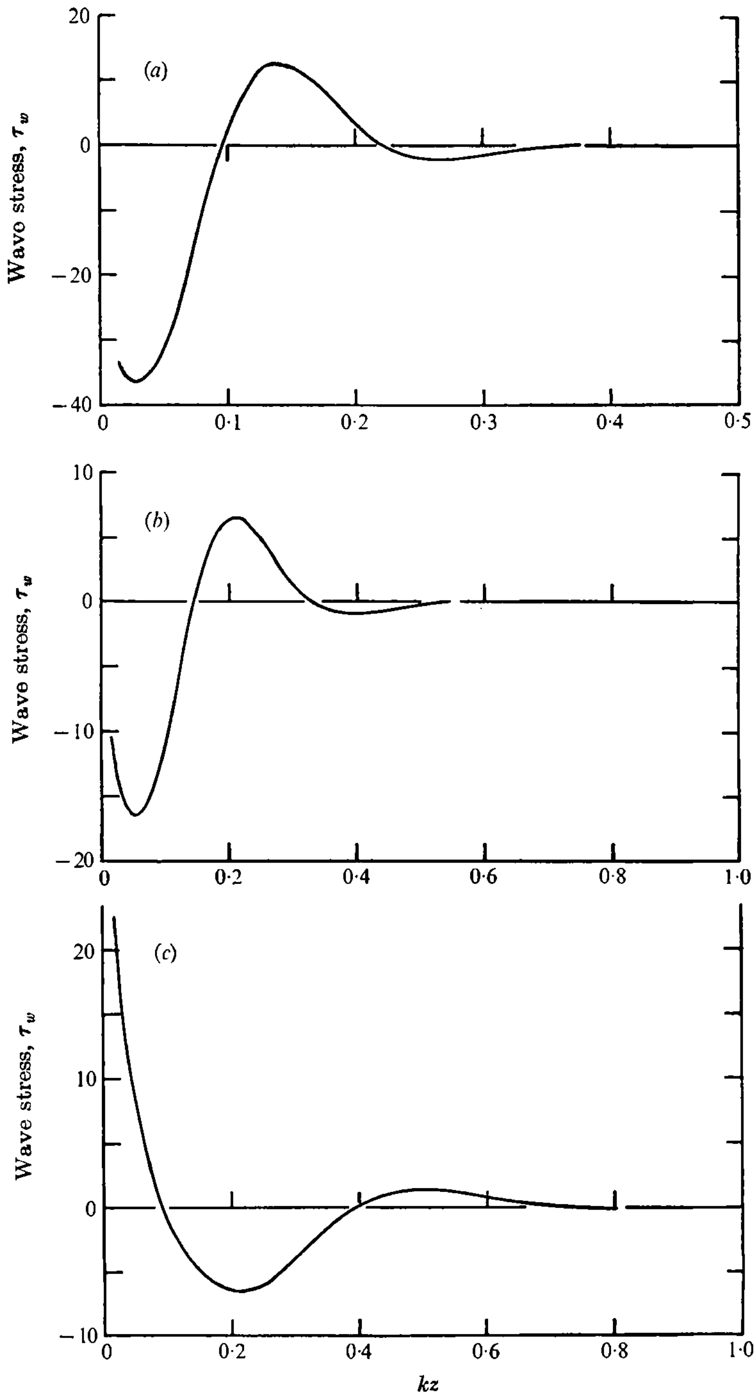

FIGURE 6. Variation of wave stress with distance from surface for $R = 10$ and (*a*) $C = 4$, (*b*) $C = 10$ and (*c*) $C = 16$. Stress is made non-dimensional with units $\tau_0(kh_0)^2$.

Reynolds 1970). In fact, use of the energy equation immediately introduces a visco-elastic response with a relaxation time as large as is plausible, and it seems unlikely that theories using linearized equations can describe the observations.

In the previous section, it was pointed out that two kinds of nonlinear behaviour become significant for wave slopes greater than 0·1. The first arises when the amplitude of the Reynolds stress becomes a considerable fraction of the average stress, and its effect is to cause vertical displacements of streamlines and of the critical surface that are large compared with distance from the surface and the wave displacement. In effect, the 'cats-eye' patterns of recirculating flow are no longer thin and they cause large displacements of the flow above them as if the flow had separated from the surface. The second depends on the fraction of the total shear stress that is transmitted by the wave-induced motion. It becomes significant for maximum wave slopes above 0·1, and it is particularly interesting that Dobson finds that the wave stress forms as much as 80 % of the total stress.

Substantial changes in the stress carried by the turbulent motion must induce considerable departures of the horizontally averaged velocity from the logarithmic distribution. An estimate may be obtained from the turbulent energy equation averaged over a complete wave:

$$\tau_\infty d\overline{U}/dz - d(\overline{pw} + \tfrac{1}{2}\overline{q^2 w})/dz = \epsilon, \tag{5.1}$$

where p, u, v and w now mean the sum of the turbulent and wave-induced fluctuations. The energy dissipation is entirely dependent on the turbulent motion and so, making the usual assumption of similarity,

$$\epsilon = \tau_0^{\frac{3}{2}}/Kz, \tag{5.2}$$

where $\tau_0 = \tau_\infty - \tau_w$ is the part of the total stress τ_∞ carried by the turbulent motion. Ignoring the diffusion term, we find that

$$\frac{d\overline{U}}{dz} = \frac{\tau_\infty^{\frac{1}{2}}}{Kz}\left(1 - \frac{\tau_w}{\tau_\infty}\right)^{\frac{3}{2}} \tag{5.3}$$

and

$$\frac{d^2\overline{U}}{dz^2} = -\frac{\tau_\infty^{\frac{1}{2}}}{Kz^2}\left(1 + \frac{3}{2}\frac{z}{\tau_\infty}\frac{d\tau_w}{dz}\right). \tag{5.4}$$

Inspection of the profiles in figure 6 shows that the curvature of the averaged velocity profiles is changed by large amounts for $kh_0 = 0{\cdot}1$ and may be reversed for slightly larger wave slopes.

The most straightforward way of extending the calculations to waves of finite amplitude is to follow Stuart (1958) and to suppose that the pattern of the velocity variations remains the same, but to use the wave stresses to determine a modified profile of horizontally averaged velocity. It is possible that a calculation similar to that described but with the modified velocity and stress distributions would lead to larger quadrature components of the pressure.

I should like to thank Prof. M. S. Longuet-Higgins for assistance and propulsion.

REFERENCES

BARNETT, T. P. & WILKERSON, J. C. 1967 *J. Mar. Res.* **25**, 417.

BRADSHAW, P., FERRISS, D. H. & ATWELL, N. P. 1967 *J. Fluid Mech.* **28**, 593.

DAVIS, R. E. 1972 *J. Fluid Mech.* **52**, 287.

DOBSON, F. W. 1971 *J. Fluid Mech.* **48**, 91.

HUSSAIN, A. K. M. F. & REYNOLDS, W. C. 1970 *Dept. Mech. Engng, Stanford Univ. Rep.* FM 6.

MILES, J. W. 1957 *J. Fluid Mech.* **3**, 185.

MILES, J. W. 1959 *J. Fluid Mech.* **6**, 568.

PHILLIPS, O. M. 1957 *J. Fluid Mech.* **2**, 417.

SNYDER, R. L. & COX, C. S. 1966 *J. Mar. Res.* **24**, 141.

STUART, J. T. 1958 *J. Fluid Mech.* **4**, 1.

TOWNSEND, A. A. 1961 *J. Fluid Mech.* **11**, 97.

TOWNSEND, A. A. 1970 *J. Fluid Mech.* **41**, 13.